Theory of fermion exchange in massive quantum electrodynamics at high energy. I*

Barry M. McCoy†
The Institute for Theoretical Physics, State University of New York at Stony Brook, Stony Brook, New York 11794

Tai Tsun Wu
Gordon McKay Laboratory, Harvard University, Cambridge, Massachusetts 02138

(Received 4 August 1975)

We consider the high-energy behavior of Compton scattering near the backward direction and of pair annihilation into two photons in massive quantum electrodynamics. We study the limit where s, the center-of-mass energy squared, becomes large and t, the square of the momentum transfer, is fixed and spacelike. In each order of perturbation theory we calculate the leading terms in the $s \to \infty$ expansion, and then these leading terms are summed. In the positive-signature channel this leads to a Regge pole. In the negative-signature channel the amplitude is dominated by a pole when $-t$ is sufficiently small. However, as $-t$ increases the pole moves to the left and eventually the amplitude is dominated by the fixed Mandelstam cut. In this paper we present the results of our calculations, summarize the most important features of the calculations, and discuss the physics of the result. The details of the calculations are presented in the 5 succeeding papers.

I. CONCLUSION

In this series of papers,[1-5] we consider the high-energy behavior for fermion-exchange processes in massive quantum electrodynamics, i.e., the field theory where a photon field A_μ of mass $\lambda > 0$ and an electron field ψ of mass m interact via the coupling $g\bar{\psi}\gamma_\mu\psi A_\mu$. More precisely, we study the two closely related problems of Compton scattering near the backward direction and pair annihilation. The kinematics for these two processes are given in Fig. 1.

We define the usual Mandelstam variables

$$s = (r_2 + r_3)^2 \tag{1.1}$$

and

$$t = (2r_1)^2 \tag{1.2}$$

and study the high-energy limit $s \to \infty$ with t fixed such that $t \leq 0$. [We use the metric $(+---)$. For γ matrixes and Feynman rules we use the conventions of Bjorken and Drell.[6]] In this limit, the only nonvanishing components of r_1 are transverse, i.e., $2r_1 \sim (0, \vec{\Delta}, 0)$.

We let $\tilde{\mathfrak{M}}_{\mu\nu}(s, r_1)$ be the backward Compton amplitude and $\bar{\mathfrak{M}}_{\mu\nu}(s, r_1)$ be the pair-annihilation amplitude. We further define $\tilde{\mathfrak{M}}(s, r_1)$ and $\bar{\mathfrak{M}}(s, r_1)$ by

$$\tilde{\mathfrak{M}}_{\mu\nu}(s, r_1) = \bar{u}(r_3 + r_1)\gamma_\mu \tilde{\mathfrak{M}}(s, r_1)\gamma_\nu u(r_2 - r_1) \tag{1.3a}$$

and

$$\bar{\mathfrak{M}}_{\mu\nu}(s, r_1) = \bar{v}(r_3 + r_1)\gamma_\mu \bar{\mathfrak{M}}(s, r_1)\gamma_\nu u(r_2 - r_1)\,. \tag{1.3b}$$

(In passing from $\tilde{\mathfrak{M}}_{\mu\nu}$ and $\bar{\mathfrak{M}}_{\mu\nu}$ to $\tilde{\mathfrak{M}}$ and $\bar{\mathfrak{M}}$ we note that we are removing a factor of $s^{1/2}$ contained in the spinors.) From $\tilde{\mathfrak{M}}$ and $\bar{\mathfrak{M}}$ we define the positive-signature amplitude as

$$\mathfrak{M}_+(s, r_1) = \tilde{\mathfrak{M}}(s, r_1) + \bar{\mathfrak{M}}(s, r_1) \tag{1.4a}$$

and the negative-signature amplitude as

$$\mathfrak{M}_-(s, r_1) = \tilde{\mathfrak{M}}(s, r_1) - \bar{\mathfrak{M}}(s, r_1)\,. \tag{1.4b}$$

In each order of perturbation theory we will, in the sequel, compute the leading behavior of the

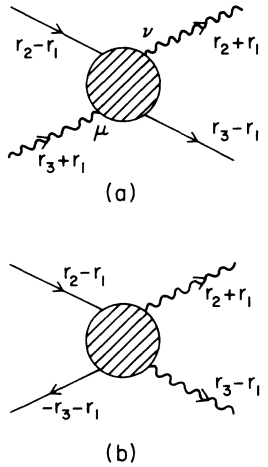

FIG. 1. (a) Kinematics for the process of Compton scattering near the backward direction. (b) Kinematics for the process of electron-positron pair annihilation into two photons.

amplitude as $s \to \infty$ with t fixed. We then sum these leading contributions over all orders. A convenient way both for carrying out the summation and for describing the result is to use the Mellin transform defined by

$$\overline{\mathfrak{M}}_{\pm}(\zeta) = \int_0^\infty ds\, s^{-\zeta-1}\mathfrak{M}_{\pm}(s)\,. \tag{1.5}$$

The behaviors of $\overline{\mathfrak{M}}_{\pm}(\zeta)$ for small ζ determine the asymptotic behaviors for $\mathfrak{M}_{\pm}(s)$ in the limit of large s.

In this approximation of summing the leading terms, the conclusions of our study are as follows:

1. For the positive-signature amplitude

$$\overline{\mathfrak{M}}_{+}(\zeta) \sim \frac{g^2}{\not\Delta + m}\,\frac{1}{1-\zeta^{-1}\alpha(\vec{\Delta})}\,[2\zeta^{-1} - \pi i\alpha(\vec{\Delta})], \tag{1.6}$$

where

$$\alpha(\vec{\Delta}) = g^2(\not\Delta + m)\int \frac{d^2\vec{k}_\perp}{8\pi^3}\,\frac{1}{\vec{k}_\perp^{\,2}+\lambda^2}\,\frac{\not\Delta + \not k_\perp - m}{(\vec{\Delta}+\vec{k}_\perp)^2+m^2}\,. \tag{1.7}$$

2. For the negative-signature amplitude

$$\overline{\mathfrak{M}}_{-}(\zeta) \sim \frac{-g^2\pi i}{\not\Delta + m}\,\frac{-\zeta^{-1}\alpha(\vec{\Delta}) + (\not\Delta + m)\Sigma_3(\vec{\Delta};\zeta)}{1+\zeta^{-1}\alpha(\vec{\Delta}) - (\not\Delta + m)\Sigma_3(\vec{\Delta};\zeta)}\,, \tag{1.8}$$

where

$$\Sigma_3(\vec{\Delta};\zeta) = i\pi^{-1}\zeta^{-1}\int \frac{d^2\vec{k}_\perp}{8\pi^3}\,\frac{1}{\vec{k}_\perp^{\,2}+\lambda^2}\,\alpha(\vec{k}_\perp + \vec{\Delta})f(\vec{k}_\perp;\zeta) \tag{1.9}$$

and $f(\vec{k}_\perp;\zeta)$ is determined from

$$[1-\zeta^{-1}\alpha(\vec{\Delta}+\vec{k}_\perp)]f(\vec{k}_\perp;\zeta) = -2\pi i g^2\zeta^{-1}\frac{1}{\not\Delta + \not k_\perp + m} + \zeta^{-1}g^2\int \frac{d^2\vec{k}'_\perp}{8\pi^3}\,\frac{1}{\vec{k}'^{\,2}_\perp+\lambda^2}\,\frac{\not\Delta + \not k_\perp + \not k'_\perp - m}{(\vec{\Delta}+\vec{k}_\perp+\vec{k}'_\perp)^2+m^2}\,(\not\Delta + \not k'_\perp + m)f(\vec{k}'_\perp;\zeta)\,. \tag{1.10}$$

II. PLAN OF PRESENTATION

The calculations which lead to these conclusions are both long and exquisite. The length is attested to by the fact that in sixth order we consider 4 Feynman diagrams, in eighth order we consider 12, in tenth order we consider 41, and in twelfth order we consider 142. The calculation is exquisite because new and intricate features appear in each of the above-mentioned orders.

Both the length and the elaborateness of this problem force us to depart from the conventional methods of presentation. It is patently unrealistic to use the Aristotelian method of first presenting the beginning, then the middle and finally the end. We will instead present our calculation as follows: In Sec. III of this paper we will discuss the history of this problem and our physical motivation for considering it. Then in Sec. IV we will discuss in an illustrative fashion some of the important points of the calculation. However, the detailed and complete calculations will be deferred to the subsequent papers of the series. We conclude this paper in Sec. V with a discussion of the physical implications of our results. It is therefore hoped that the reader can appreciate both the physics of our results and the principles of the mathematical methods which go into its derivation without being oppressed by the details.

It is, however, mandatory that the details of our calculation be presented, and this is done in the 5 following papers. In the end there is no substitute for the real thing and no amount of general discussion is a substitute for the explicit calculation. The crucial question in investigations of this sort in this: "How do you know that you have actually found all contributions to the final result?" There exist many errors in the literature where, in fact, there are more contributions than those found by investigators. In all those cases the papers become vague and the reader is asked to accept the author's answer to the above question on faith. We hope, by displaying our explicit calculations in detail, to demonstrate to the reader that our final results rest on sound calculations.

III. HISTORY AND PHYSICAL MOTIVATION

The study of the high-energy behavior of fermion exchange in massive quantum electrodynamics by the method of extracting the largest term in each order of perturbation theory and then computing the sum was initiated in 1964 by Gell-Mann, Goldberger, Low, Marx, and Zachariasen.[7] Previous to this study it had been shown[8] in ϕ^3 theory that this procedure of summing leading terms leads to an amplitude of the form (see Fig. 2)

$$\beta(t)s^{\alpha_\phi(t)}\,, \tag{3.1}$$

where

$$\alpha_\phi(t) = -1 + g^2\int \frac{d^2\vec{k}_\perp}{16\pi^3}\,\frac{1}{\vec{k}_\perp^{\,2}+m^2}\,\frac{1}{(\vec{\Delta}-\vec{k}_\perp)^2+m^2}\,. \tag{3.2}$$

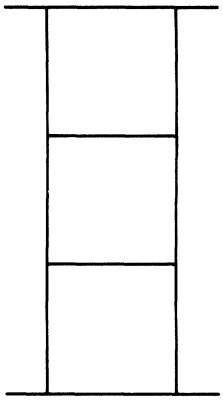

FIG. 2. A ladder diagram in ϕ^3 theory.

In order to see whether results such as (3.1) obtain when a quantum number is exchanged, Gell-Mann, Goldberger, Low, Marx, and Zachariasen studied fermion exchange in fourth-order perturbation theory. They found that in the backward Compton channel, with $\alpha(\vec{\Delta})$ as defined by (1.7),

$$\tilde{\mathfrak{M}}^{(4)} \sim g^2 \ln s \frac{\alpha(\vec{\Delta})}{\not{\Delta} + m} , \tag{3.3a}$$

while in the pair-annihilation channel

$$\bar{\mathfrak{M}}^{(4)} \sim g^2 (\ln s - \pi i) \frac{\alpha(\vec{\Delta})}{\not{\Delta} + m} . \tag{3.3b}$$

They then continued to the sixth-order perturbation theory. With their Feynman-parameter methods they found the calculation much more formidable than in fourth-order. In particular they found that the three diagrams of Fig. 3 each give $\ln^3 s$ and not the $\ln^2 s$ which one might expect. However, they quote an unpublished calculation of Federbush to the effect that the offending $\ln^3 s$ terms cancel and that one is left in the backward Compton channel with

$$g^2 \tfrac{1}{2} (\ln s - \pi i)^2 \frac{\alpha^2(\vec{\Delta})}{\not{\Delta} + m} \tag{3.4a}$$

and in the pair-annihilation channel with

$$g^2 \tfrac{1}{2} \ln^2 s \frac{\alpha^2(t)}{\not{\Delta} + m} . \tag{3.4b}$$

On the basis of these calculations Gell-Mann, Goldberger, Low, Marx, and Zachariasen make the following conjecture: In $(4n+2)$-order perturbation theory the leading behavior of the backward Compton amplitude is

$$\tilde{\mathfrak{M}}^{(4n+2)} \sim g^2 \frac{1}{(2n)!} (\ln s - \pi i)^{2n} \frac{\alpha^{2n}(t)}{\not{\Delta} + m} \tag{3.5a}$$

and that for pair annihilation is

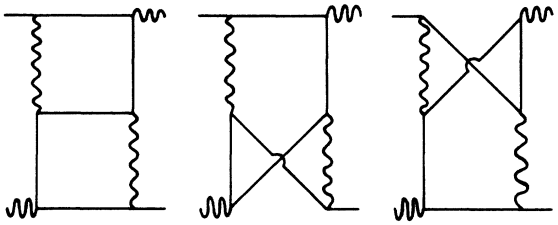

FIG. 3. Three diagrams which contribute to the backward Compton amplitude in sixth order. Each one of these diagrams is separately of order $\ln^3 s$ but the sum is of order $\ln^2 s$.

$$\bar{\mathfrak{M}}^{(4n+2)} \sim g^2 \frac{1}{(2n)!} \ln^{2n} s \frac{\alpha^{2n}(t)}{\not{\Delta} + m} . \tag{3.6a}$$

In $4n$-order perturbation theory the backward Compton amplitude is

$$\tilde{\mathfrak{M}}^{(4n)} \sim g^2 \frac{1}{(2n-1)!} \ln^{2n-1} s \frac{\alpha^{2n-1}(t)}{\not{\Delta} + m} \tag{3.5b}$$

and the pair-annihilation amplitude is

$$\bar{\mathfrak{M}}^{(4n)} \sim g^2 \frac{1}{(2n-1)!} (\ln s - \pi i)^{2n-1} \frac{\alpha^{2n-1}(t)}{\not{\Delta} + m} . \tag{3.6b}$$

When these leading-order conjectures are summed they obtain, for the amplitudes (1.4),

$$\mathfrak{M}_+ \sim \frac{g^2}{\not{\Delta} + m} [1 + e^{-\pi i \alpha(\vec{\Delta})}] s^{\alpha(\vec{\Delta})} \tag{3.7a}$$

and

$$\mathfrak{M}_- \sim \frac{g^2}{\not{\Delta} + m} [1 - e^{\pi i \alpha(\vec{\Delta})}] s^{-\alpha(\vec{\Delta})} . \tag{3.7b}$$

These are very strange results.

The difficulty with these results is seen most strikingly if we let $-t$ become large. Then from (1.10)

$$\alpha(t) \sim \frac{-g^2}{8\pi^2} \ln |t| . \tag{3.8}$$

For the positive-signature amplitude (3.7a) such a behavior is fine. However, for the negative-signature amplitude it means that for sufficiently large $-t$ (3.7b) will violate unitarity.

Stated more phenomenologically, (3.7) says that if in the positive-signature channel the amplitude falls off more rapidly with increasing s when $-t$ is increased, then the negative-signature amplitude falls off *less* rapidly with increasing s when $-t$ is increased. Such behavior has never been seen experimentally.

A year later in 1965 a more detailed Feynman-parameter calculation of the $s \to \infty$ behavior of the sixth-order amplitude was carried out.[9] It was shown there that in addition to the diagrams of Fig. 3 which contribute to order $\ln^3 s$ and to order $\ln^2 s$ the 6 diagrams of Fig. 4 must be included since they also contribute to order $\ln^2 s$. However, after summing all these diagrams the result of (3.4) was obtained (to order $\ln^2 s$).

Further progress was made in 1967 with the work of Frolov, Gorshkov, and Gribov[10] who studied backward Compton scattering in the massless case $\lambda = 0$. As a byproduct of their calculation, in Appendix B they discuss the case $\lambda \neq 0$. and claim to obtain the leading term in (3.5). However, in their calculation in $(2n+2)$-order perturbation theory they calculate $2^n - 1$ diagrams, which does not agree with the 9 diagrams needed in sixth-order to obtain (3.4).

After 1967 attention was shifted away from fermion exchange. In 1970 the results were published[11] of a massive study of a related process, namely elastic scattering in quantum electrodynamics. Here it was discovered that the total cross section rises as $\ln^2 s$ as $s \to \infty$ and that elastic scattering is describable as the scattering from a black disk whose radius increases with energy. This rising of elastic cross sections was observed in hadron scattering at CERN ISR in 1973[12] and also at Fermilab in 1974.[13]

In this study of elastic scattering it was learned that the $s \to \infty$ limit may be studied in momentum space more conveniently than it is studied in Feynman-parameter space. This insight is very useful for this present problem because of the extreme difficulty already encountered in sixth order in the use of Feynman parameters. Moreover, data for quantum-number exchange processes will soon become available at Fermilab at the energies where the rising elastic cross sections are seen. Because of the increases in our calculational abilities and because of the imminent prospect of obtaining high-energy quantum-number exchange data it seems to be an opportune time to restudy the problem of fermion exchange and, in particular, to demonstrate that the peculiar conjecture (3.7b) is to be replaced by the results (1.8)–(1.10).

IV. DISCUSSION OF THE CALCULATION

With the foregoing discussion of the background of our problem we may now proceed to discuss the calculations we have done. This we will do in the following subsections.

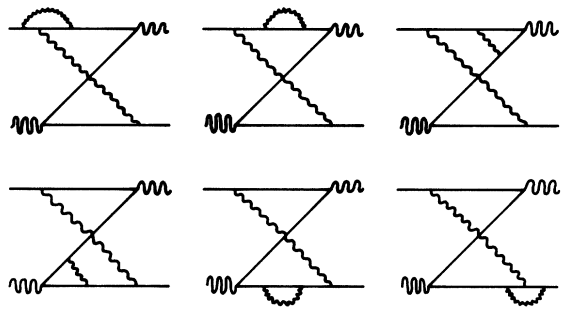

FIG. 4. Six more diagrams which must be included with the diagrams of Fig. 3 to obtain the correct answer for the sixth-order backward Compton scattering. Each of these diagrams is of order $\ln^2 s$.

A. The meaning of $\ln^n s$ and $(\ln s - \pi i)^n$

It must first be recognized that in expressions such as (3.5) and (3.6) there is a world of difference between the statement that the leading term is

$$\ln^n s \tag{4.1}$$

and the statement that the leading term is

$$(\ln s - \pi i)^n \tag{4.2}$$

The first statement may perhaps be interpreted to mean that as $s \to \infty$ the amplitude behaves as

$$\ln^n s + O(\ln^{n-1} s)\ , \tag{4.3}$$

but how is the second statement to be interpreted? Surely the two most obvious interpretations of (4.2), namely

$$(\ln s - \pi i)^n + o(1) \tag{4.4a}$$

and

$$(\ln s - \pi i)^n + O((\ln s - \pi i)^{n-1})\ , \tag{4.4b}$$

are both incorrect. The first interpretation is false because for large n the calculations are not that accurate. The second interpretation is wrong because (4.4b) is mathematically identical to $\ln^n s + O(\ln^{n-1} s)$.

Our first step, therefore, is to analyze the calculations in fourth and sixth order to see what the meaning of (4.1) and (4.2) should be. This is done in the next paper[1] and we see explicitly that both (4.3) and (4.4) are incorrect. Instead, we find that in general for $(2n+2)$-order perturbation theory the leading imaginary part of the amplitude is of order $\ln^{n-1} s$. (For the purpose of this statement the γ matrices are considered to be real.) We are

able to compute both of these leading real and leading imaginary parts even though the imaginary part is one power of ln$s$ smaller than the real part. Therefore, (4.1) *means that the real part is* $\ln^n s + O(\ln^{n-1} s)$ *and that the imaginary part is smaller than* $\ln^{n-1} s$, *while in* (4.2) *the real and imaginary parts are respectively*

$$\ln^n s + O(\ln^{n-1} s) \tag{4.5a}$$

and

$$-n\pi \ln^{n-1} s + O(\ln^{n-2} s). \tag{4.5b}$$

It is also readily seen that in $(2n+2)$-order perturbation theory (for $n \geq 1$), the leading terms of a backward Compton diagram and the corresponding pair-annihilation diagram are related by the substitution

$$\ln^n s \to \ln^n s - n\pi i \ln^{n-1} s .$$

Therefore, while for the positive-signature amplitude it suffices to compute the leading real part, *for the negative-signature amplitude the leading real parts cancel and the entire result comes from the leading imaginary part of the amplitude.*

B. Transverse cutoff

We have learned, from the case of elastic scattering in massive quantum electrodynamics[14] that high-order calculations are best carried out in momentum space instead of Feynman-parameter space. This procedure involves the introduction of a cutoff $k_{\max}$ in transverse momentum, carrying out the asymptotic computation $s \to \infty$ with a finite value of $k_{\max}$, adding up the contributions from various diagrams, and finally letting $k_{\max}$ increase without bound. *We are, in effect, interchanging the limits* $k_{\max} \to \infty$ *and* $s \to \infty$.

Since this procedure works successfully in the case of elastic scattering, it is expected to work also for the present case of fermion exchange. In the next paper, we apply this method to calculate the sixth-order case in momentum space (as Frolov, Gorshkov, and Gribov[10] did). With a finite $k_{\max}$, the three diagrams of Fig. 3 are each of order $\ln^2 s$ instead of $\ln^3 s$. For each diagram, the coefficient of $\ln^2 s$ is an integral over the transverse momenta which diverges as $k_{\max} \to \infty$. However, if we add the amplitudes of all three diagrams together, the divergences cancel in the $k_{\max} \to \infty$ limit and we are left with a convergent result. Furthermore, this result is the same as that obtained by the more honest Feynman-parameter calculation.

This consideration explains the puzzle as to how many diagrams contribute to the leading real terms in sixth order. If a transverse cutoff is not used, we need all nine diagrams in Fig. 3 and Fig. 4. If a transverse cutoff is used, it suffices to take the three diagrams of Fig. 3 into account, since the six diagrams of Fig. 4 are only of order ln$s$ for finite $k_{\max}$. More generally, with this method of transverse cutoff, we have exactly as many diagrams contributing to the leading real part as do Frolov, Gorshkov, and Gribov.

C. Imaginary part of sixth-order diagrams

Thus far we have merely refined our understanding of the details of the previous calculations.[7,10] However, once it is realized that in order to compute the negative-signature amplitude correctly it is necessary to calculate the leading imaginary part as well as the leading real part, we see[1] that the sixth-order results (3.4) are in serious error.

The result (3.4) has omitted the diagram of Fig. 5.

For backward Compton scattering the diagram of Fig. 5 gives the leading contribution of

$$g^6 \pi i \ln s \int \frac{d^2\vec{k}_{1\perp}}{8\pi^3} \frac{d^2\vec{k}_{2\perp}}{8\pi^3} \frac{1}{\vec{k}_{1\perp}^{\,2} + \lambda^2} \frac{1}{\vec{k}_{2\perp}^{\,2} + \lambda^2} \times \frac{-\vec{k}_{1\perp} - \vec{k}_{2\perp} - \vec{\Delta} + m}{(\vec{k}_{1\perp} + \vec{k}_{2\perp} + \vec{\Delta})^2 + m^2} . \tag{4.6}$$

This is purely imaginary and hence does not affect the real part of order $\ln^2 s$. Furthermore, the corresponding graph for pair annihilation is precisely the negative of (4.6) and hence this new term does not affect the positive-signature amplitude.

But (4.6) will contribute to the negative-signature amplitude. Therefore the peculiar statement of (3.7b) is incorrect.

D. Salient features of the eighth-order calculation

In the third paper of this series[2] we examine eighth-order perturbation theory. We find that in addition to the 7 diagrams of Frolov, Gorshkov, and Gribov[7] which contribute to the leading real

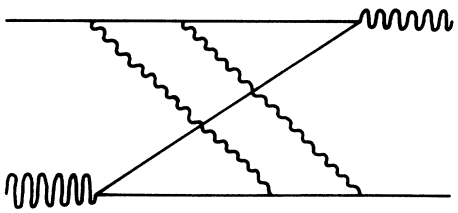

FIG. 5. A fourth diagram which contributes to the leading imaginary part of the sixth-order amplitude for backward Compton scattering.

part there are 5 additional diagrams which contribute to the leading imaginary part but do not contribute to the leading real part. Each of these 12 diagrams is of order $\ln^3 s$ or $i\ln^2 s$ and when added together the cutoff $k_{\max}$ may be removed and a finite result obtained. But now the cancellation is much more elaborate than in sixth order. The 12 contributing diagrams in the backward Compton channel are shown in Fig. 6. The first 7 of these contribute to the real part of order $\ln^3 s$ and when summed give a result in which the $k_{\max} \to \infty$ limit may be taken. But while diagrams 1–5 do not have an imaginary part of order $\ln^2 s$, diagrams 6 and 7 do. Therefore, in the imaginary part coming from diagrams 1–7 the cutoff $k_{\max}$ cannot be removed. However, this extra imaginary part coming from diagrams 6 and 7 is precisely what is needed to add to the sum of diagrams 8–12 to allow the cutoff to be removed. Thus we see that all the diagrams 1–12 must be included before the cutoff may be removed in both the real and imaginary parts.

There are, of course, many eighth-order diagrams other than those of Fig. 6. Some of these are shown in Fig. 7. None of these other diagrams contribute to either the leading real or imaginary part.

E. Salient features of the tenth-order calculation

In the fourth paper of this series[3] we discuss tenth-order perturbation theory. Here there are 41 diagrams which contribute and they are all tied

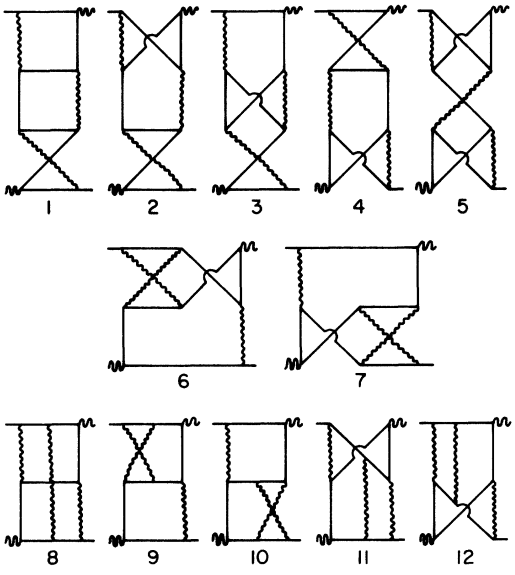

FIG. 6. The 12 diagrams which contribute to the leading real and leading imaginary parts of the eighth-order amplitude for backward Compton scattering.

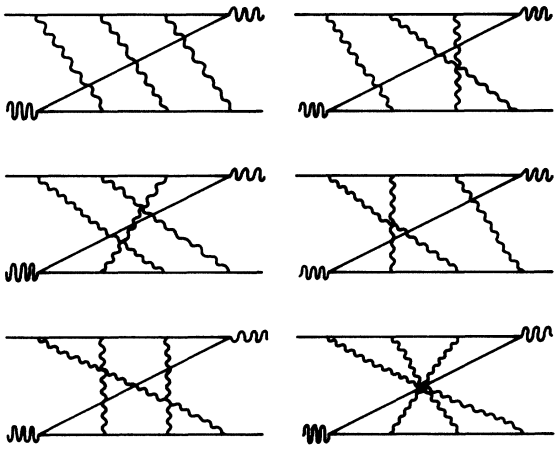

FIG. 7. Six diagrams which do not contribute to the leading real or imaginary parts of the eighth-order amplitude for backward Compton scattering.

together in a complicated cancellation which allows the $k_{\max} \to \infty$ limit to be taken. If any one of these diagrams is omitted, the $k_{\max}$ cutoff cannot be removed. Indeed, the non-Mandelstam diagrams which we discussed in ϕ^3 theory[15] were found because their counterparts in this problem are needed to allow the cutoff to be removed.

There are actually 3 classes of diagrams in tenth order, not 2. In addition to the diagrams (1) which contribute to the leading real part and the diagrams (2) which contribute to the leading imaginary part but not the leading real part we distinguish that subclass of class 2 whose leading imaginary parts identically cancel out; such pairs of cancelling diagrams are shown in Fig. 8.

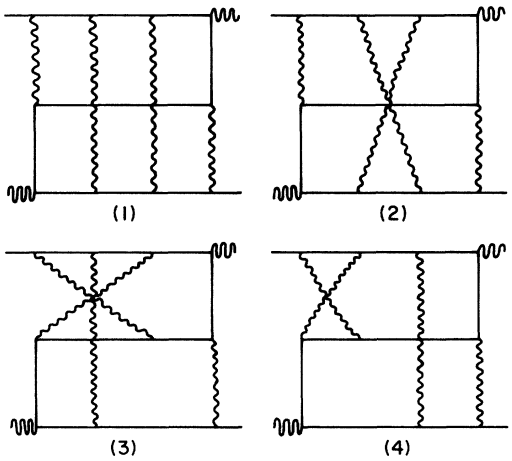

FIG. 8. Four diagrams whose contributions to the leading imaginary part of the tenth-order backward Compton amplitude cancel out. The diagrams 1 and 2 cancel and the diagrams 3 and 4 cancel.

F. Transverse diagrams

It is useful to introduce the notation in $2n+2$ order of perturbation theory:

$$(m_1, m_2) = \frac{1}{n!}[m_1 \ln^n s + m_2(\ln^n s - n\pi i \ln^{n-1} s)]. \quad (4.7)$$

In this notation a diagram for backward Compton scattering and the corresponding diagram for pair annihilation are (for $n \geq 1$) related by

$$(m_1, m_2)_{\text{backward Compton}} = (m_2, m_1)_{\text{pair annihilation}} \quad (4.8)$$

The results of each of the previous expansions are all of the form of (m_1, m_2) times a function of $\vec{\Delta}$ which can be represented as an integral in the space of two-dimensional transverse momenta with an integrand which can be represented by a diagram in this transverse-momentum space. Moreover, after the Feynman diagrams are combined and the $k_{\max} \to \infty$ limit taken, the result still has a diagrammatic representation in transverse-momentum space. For the transverse diagrams of the final combined amplitudes we have the following rules:

(1) For each photon line of momentum $\vec{k}_\perp$ there is a propagator

$$(\vec{k}_\perp^{\,2} + \lambda^2)^{-1}. \quad (4.9)$$

(2) For each election line of momentum $\vec{k}$ there is a propagator

$$\frac{\vec{k}_\perp + m}{k_\perp^{\,2} + m^2}. \quad (4.10)$$

(3) For each internal vertex through which there flows a momentum $\vec{k}_\perp$ there is a factor

$$\vec{k}_\perp - m. \quad (4.11)$$

(4) Each independent momentum is integrated over using

$$\int d^2\vec{k}_\perp (2\pi)^{-3}. \quad (4.12)$$

The results of fourth-, sixth-, eighth-, and tenth-order perturbation theory are thus succinctly summarized in terms of the transverse diagrams of Fig. 9. In this figure we display the diagrams and the associated pairs (m_1, m_2) for backward Compton scattering. As an example of the rules we note that the result corresponding to the second sixth-order diagram of Fig. 9 is explicitly written out in (4.6).

G. Twelfth and higher-order results

Unfortunately, the results of fourth- through tenth-order perturbation theory are not quite sufficient to generalize to higher order. This is in part because in twelfth order there are triplets and quartets of diagrams which cancel each other in addition to the pairs of cancelling diagrams found in tenth order. In higher orders the situation is even more complicated and the nonexistence of certain possible transverse diagrams follows from the cancellation of a large number of Feynman diagrams (whose number increases with the order of perturbation theory). Therefore, in the fifth paper of this series[4] we consider in detail twelfth-order perturbation theory and introduce a matrix method which allows us to rapidly calculate the contribution of large classes of diagrams in an arbitrary order of perturbation theory. We show there, for example, that the Feynman diagram of Fig. 10(a) does not contribute to leading order [and hence that the transverse diagram Fig. 10(b) is absent]. We also show that the diagram of Fig. 11(a) does contribute. However, when we consider all diagrams made up of layers which contain either two crossed photons or two parallel photons such as Fig. 11(b) then the complete sum of this class does not contribute to tenth or higher order. Other Feynman diagrams which are shown to vanish to leading imaginary order when summed are given in Fig. 12.

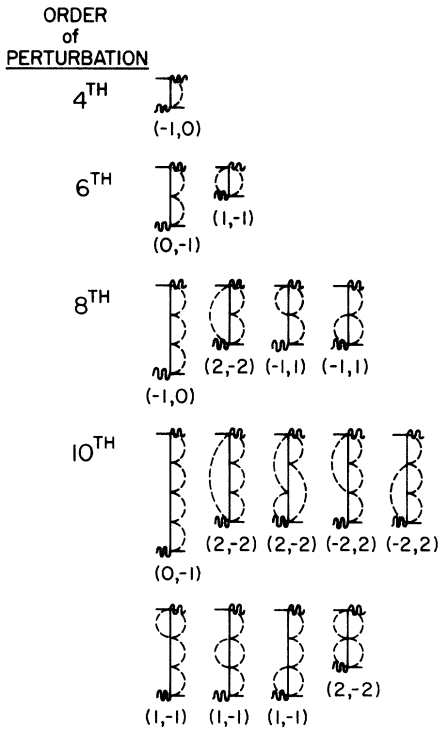

FIG. 9. The transverse diagrams and their pairs (m_1, m_2) which contribute to the backward Compton amplitude in fourth, sixth, eighth, and tenth order.

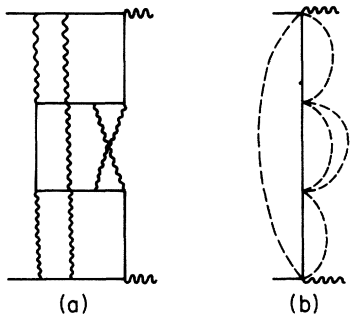

FIG. 10. (a) A twelfth-order Feynman diagram which does not contribute to the leading real or imaginary part of the pair-annihilation amplitude. (b) The transverse diagram corresponding to Fig. 10(a).

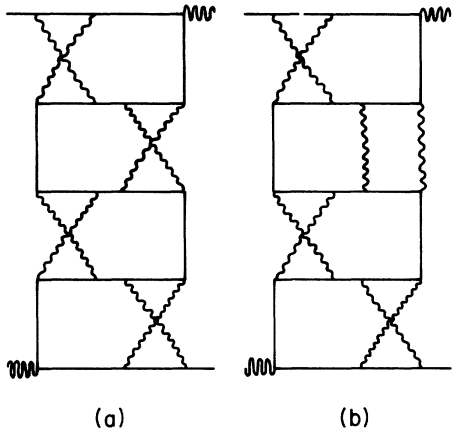

FIG. 11. The eighteenth-order Feynman diagrams which exemplify a cancellation discussed in the text.

H. The final answer

From these calculations we find that the following rules hold (for the backward Compton channel):

(1) Each transverse diagram is made up of a number of segments, each of which may contain either two-particle states or three-particle states but not four-or-more particle states.

(2) Three-particle segments may be next to each other and do *not* have to (although they may) be separated by one or more two-particle segments,

(3) If the transverse diagram consists of n two-particle electron-photon bubbles the contribution is

$$(-1, 0) \text{ if } n \text{ is odd}, \tag{4.13a}$$

$$(0, -1) \text{ if } n \text{ is even}. \tag{4.13b}$$

(4) If in $2n+2$ order the transverse diagram consists of only one three-particle segment, then the contribution is

$$(2, -2) \text{ if } n \geq 3, \tag{4.14a}$$

$$(1, -1) \text{ if } n = 2. \tag{4.14b}$$

(5) If the transverse diagram is made up of a number of segments with 2 or 3 particles and if the contribution from the i^{th} three-particle segment by itself in $(2n_i+2)$-order perturbation theory is $(m_i, -m_i)$ and if N_2 is the total number of two-particle electron-photon bubbles in the diagram, then the contribution from the entire diagram is

$$(-1)^{N_2}\tfrac{1}{2}\left\{\prod_i (2m_i),\ -\prod_i (2m_i)\right\}. \tag{4.15}$$

In the final paper of this series[5] we sum the leading terms in each order of perturbation theory and obtain the results quoted in Sec. I.

V. DISCUSSION OF RESULTS

It remains to discuss the physics contained in the results (1.8)–(1.13).

First of all, we remark that the amplitudes $\mathfrak{M}_+(\zeta)$ and $\mathfrak{M}_-(\zeta)$ are still 2×2 matrices. However, the only two matrices involved are the unit matrix and $\vec{\Delta}$, and hence it is convenient to work in the basis where

$$\vec{\Delta} = -i\,|\Delta|\sigma_z \tag{5.1}$$

in diagonal. We diagonalize $\alpha(\vec{\Delta})$ by writing (1.10) in terms of Feynman parameters. Thus

$$\alpha(\vec{\Delta}) = -\frac{g^2}{8\pi^2}\int_0^1 d\alpha_1 \frac{\vec{\Delta}^2\alpha_1 + m^2}{\vec{\Delta}^2\alpha_1(1-\alpha_1)+\alpha_1\lambda^2+(1-\alpha_1)m^2} - \frac{g^2}{8\pi^2} m|\Delta| i\sigma_z \int_0^1 d\alpha_1 \frac{1-\alpha_1}{\vec{\Delta}^2\alpha_1(1-\alpha_1)+\alpha_1\lambda^2+(1-\alpha_1)m^2} \tag{5.2}$$

and we see that in general $\alpha(\vec{\Delta})$ is complex. However, when $\vec{\Delta}=0$, $\alpha(0)$ is real and we find

$$\alpha(0) = \frac{-g^2}{8\pi^2}\frac{m^2}{m^2-\lambda^2}\ln\frac{m^2}{\lambda^2}. \tag{5.3}$$

The $s\to\infty$ behavior of $\mathfrak{M}_-(s)$ as given by (1.8) is determined by the singularity of $\mathfrak{M}_-(\zeta)$ furthest to the right in the ζ plane. This singularity may be either a pole determined from

$$0 = \det[1 + \zeta^{-1}\alpha(\vec{\Delta}) - (\vec{\not{\Delta}} + m)\Sigma_3(\vec{\Delta};\zeta)] \tag{5.4}$$

or a cut from $\Sigma_3(\vec{\Delta};\zeta)$ [a pole in $\Sigma_3(\vec{\Delta};\zeta)$ will not lead to a singularity of $\overline{\mathfrak{M}}_-(\zeta)$].

It may be seen from (1.9) and (1.10) that (when the space of transverse momentum is two-dimensional) $\Sigma_3(\vec{\Delta},\zeta)$ will have a Mandelstam cut at

$$\zeta_{\text{cut}}=\alpha(0). \tag{5.5}$$

This cut is present for any value of $\vec{\Delta}$ so that to determine the behavior of $\overline{\mathfrak{M}}_-(\zeta)$ for $\vec{\Delta}$ large we must determine if these are any poles in $\overline{\mathfrak{M}}_-(\zeta)$ lying to the right of (5.5).

We study the possibility of these additional poles by defining

$$x=\frac{\zeta^{-1}g^2}{8\pi^2}\ln\vec{\Delta}^2 \tag{5.6}$$

and considering x to be of order 1 (and positive) as $\ln\vec{\Delta}^2\to\infty$. Then we find that

$$\zeta^{-1}\alpha(\vec{\Delta})\to -x \tag{5.7}$$

and Eq. (1.13) for $f(k;\zeta)$ becomes (for $|k| << |\vec{\Delta}|$)

$$(1+x)f\sim -2\pi i g^2\zeta^{-1}\not{\vec{\Delta}}^{-1}-xf. \tag{5.8}$$

Therefore $f(k;\zeta)$ is approximated by

$$f\sim -\frac{2\pi i g^2\zeta^{-1}}{\not{\vec{\Delta}}(1+2x)} \tag{5.9}$$

and hence from (1.12) we have

$$\Sigma_3(\vec{\Delta};\zeta)\sim -\frac{2x^2}{\not{\vec{\Delta}}(1+2x)}\,. \tag{5.10}$$

Using this approximation in (1.11) we find

$$\overline{\mathfrak{M}}_-(\xi)\sim -\frac{g^2\pi i}{\not{\vec{\Delta}}}(1+x)^{-1}\,. \tag{5.11}$$

This approximation has no poles lying to the right of the Mandelstam cut (5.5). Therefore, for sufficiently large $\vec{\Delta}$

$$\mathfrak{M}(s)\sim s^{\alpha(0)}\,, \tag{5.12}$$

where the $\sim$ indicates that there will be some additional power of $\ln s$ multiplying the expression.

We have thus found that our $\mathfrak{M}_+$ is given by a single moving Regge pole at $\alpha(t)$ which goes to $-\infty$ as $-t\to\infty$. This agrees with Gell-Mann, Goldberger, Low, Marx, and Zachariasen. However, we find for sufficiently large $\vec{\Delta}$ that $\mathfrak{M}_-$ is dominated by a fixed cut at $\alpha(0)$ which is vastly different from the erroneous moving Regge pole of Gell-Mann, Goldberger, Low, Marx, and Zachariasen at $-\alpha(t)$.

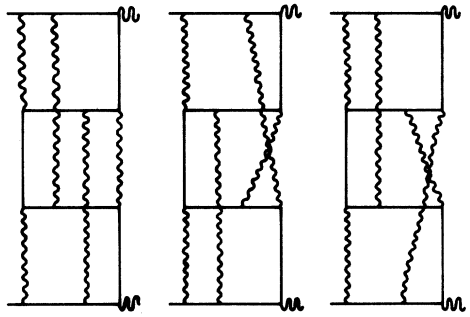

FIG. 12. Three twelfth-order Feynman diagrams whose sum does not contribute to the leading real or imaginary part.

Finally we may study the integral equation (1.10) when $\vec{\Delta}=0$. In this case it may be shown that for $m>0$ there is a pole in the amplitude $\overline{\mathfrak{M}}_-(\zeta)$ which lies to the right of the Mandelstam cut.

We therefore have the following description of the amplitude.

(a) The positive-signature amplitude $\overline{\mathfrak{M}}_+(\zeta)$ is given by a single moving Regge pole at $\zeta=\alpha(t)$ which goes to $-\infty$ as $-t\to\infty$,[16] This agrees with Gell-Mann, Goldberger, Low, Marx, and Zachariasen.

(b) The negative-signature amplitude $\overline{\mathfrak{M}}_-(\zeta)$ is dominated by a pole on the real axis when $\vec{\Delta}=0$ which becomes complex and moves to the left as $|\vec{\Delta}|$ increases. At some finite value of $-t$ the pole moves to the left of the Mandelstam cut at $\zeta=\alpha(0)$ and fixed-cut behavior is obtained for all larger values of $-t$. This behavior is very reminiscent to that of the Pomeron[12] except that in the present problem the crossover from pole to cut occurs for a physical value of t.

ACKNOWLEDGMENT

We wish to thank Professor M. L. Goldberger and Professor C. N. Yang for most useful discussions.

*Work supported in part by the U. S. Energy Research and Development Administration under Contract No. AT(11-1)-3227.

† Alfred P. Sloan fellow. Work supported in part by the National Science Foundation under Grant No. DMR730-7565 A01.

[1]B. M. McCoy and T. T. Wu, following paper, Phys. Rev. D 13, 379 (1976).

[2]B. M. McCoy and T. T. Wu, this issue, Phys. Rev. D 13, 395 (1976).

[3]B. M. McCoy and T. T. Wu, this issue, Phys. Rev. D 13, 424 (1976).
[4]B. M. McCoy and T. T. Wu, this issue, Phys. Rev. D 13, 484 (1976).
[5]B. M. McCoy and T. T. Wu, this issue, Phys. Rev. D 13, 508 (1976).
[6]J. D. Bjorken and S. D. Drell, *Relativistic Quantum Mechanics* (McGraw-Hill, New York, 1964).
[7]M. Gell-Mann, M. L. Goldberger, F. E. Low, E. Marx, and F. Zachariasen, Phys. Rev. 133, B145 (1964).
[8]J. C. Polkinghorne, J. Math. Phys. 4, 503 (1963).
[9]H. Cheng and T. T. Wu, Phys. Rev. 140, B465 (1965).
[10]G. V. Frolov, V. G. Gorshkov, and V. N. Gribov, Ann. Phys. (N. Y.) 43, 201 (1967).
[11]H. Cheng and T. T. Wu, Phys. Rev. Lett. 24, 1456 (1970).
[12]U. Amaldi, R. Biancastelli, C. Bosio, G. Matthiae, J. V. Allaby, W. Bartel, G. Cocconi, A. N. Diddens, R. W. Dobinson, and A. M. Wetherell, Phys. Lett. 44B, 112 (1973); S. R. Amendolia, G. Belletini, P. L. Braccini, C. Bradaschia, R. Castaldi, V. Cavasinni, C. Cerri, T. Del Prete, L. Foa, P. Giromini, P. Laurelli, A. Menzione, L. Ristori, G. Sanguinetti, M. Valdata, G. Finocchiaro, P. Grannis, D. Green, R. Mustard, and R. Thun, *ibid.* 44B, 119 (1973).
[13]A. S. Carroll, I-H. Chiang, T. F. Kycia, K. K. Li, P. O. Mazur, P. Mockett, D. C. Rahn, R. Rubinstein, W. F. Baker, D. P. Eartly, G. Giacomelli, P. F. M. Koehler, K. P. Pretzl, A. A. Wehmann, R. L. Cool, and O. Fackler, Phys. Rev. Lett. 33, 928 (1974); 33, 932 (1974).
[14]H. Cheng and T. T. Wu, Phys. Rev. 182, 1899 (1969).
[15]B. M. McCoy and T. T. Wu, Phys. Rev. D 12, 546 (1975).
[16]It is an extremely interesting question to ask whether this behavior for the positive-signature channel will persist if terms beyond leading logarithms are summed. We speculate that, when these nonleading terms are taken into account, fixed cuts also appear in the positive-signature channel in much the same way as in the negative-signature channel.